Relationship between the electric field variability and Poynting flux

Qingyu Zhu[1,2], Yue Deng[1], Astrid Maute[2], Arthur Richmond[2], Delores Knipp[2,3]
[1]University of Texas at Arlington, Arlington, TX, USA [2]High Altitude Observatory, National Center for Atmospheric Research, Boulder, CO, USA
[3]University of Colorado Boulder, Boulder, CO, USA

MITC-10
2017 CEDAR Workshop

Abstract: The electric field variability from an empirical model has been coupled into Global Ionosphere and Thermosphere Model (GITM) to study the impact of the electric field variability on the Joule heating. In addition, the relationship between Joule heating due to the mean electric field together with the electric variability and energy input from the magnetosphere has been examined through the comparisons between Joule heating from GITM and Poynting flux from the empirical model and Defense Meteorological Satellite Program (DMSP) F15 satellite observations. Although GITM Joule heating after including the electric variability has a significant enhancement as compared with Joule heating without the electric field variability and becomes more consistent with the distribution of Poynting flux, it is greater than Poynting flux in general, especially during the winter. The comparisons between observations and modelled results show that GITM tends to overestimate the energy input at cusp and nightside regions, while the empirical model may underestimate Poynting flux at cusp.

1. Empirical model of the electric field variability and Poynting flux

The empirical model is based on 392 DE2 satellite passes with good data quality from 1981 to 1983. DE2 satellite can provide simultaneous observations for ion drift velocity (**V**), magnetic field (**B**), therefore the electric field (**E**), magnetic field disturbance (Δ**B**) and Poynting flux (S) can be calculated by:

$$\mathbf{E} = -\mathbf{V}\times\mathbf{B_0} \qquad \Delta\mathbf{B} = \mathbf{B} - \mathbf{B_0} \qquad \mathbf{S} = \frac{\mathbf{E}\times\Delta\mathbf{B}}{\mu_0}$$

Where $\mathbf{B_0}$ is the main geomagnetic field given by the IGRF model. Then all quantities are converted to modified magnetic Apex coordinate [Richmond 1995], and mapped to the reference height at 110 km. The model can provide different quantities under different IMF clock angle, IMF strength (Bt), dipole tilt angle (T) conditions.

1.1 Electric field variability

Generally, the electric field variability can be expressed as the standard deviation of the electric field

$$\sigma(\mathbf{E}) = \sqrt{\frac{\sum_1^N (\mathbf{E_i} - \bar{\mathbf{E}})^2}{N}}$$

where $\mathbf{E} = E_{d1}\mathbf{d_1} + E_{d2}\mathbf{d_2}$ [Richmond 1995] ($\mathbf{d_1}$ represents magnetic east- and west-ward, $\mathbf{d_2}$ is magnetic north- and south-ward). $\bar{\mathbf{E}}$ is the mean electric field provided by the model.

1.2 Poynting flux

(1) (2)

$$\bar{\mathbf{S}} = \frac{\overline{\mathbf{E}\times\Delta\mathbf{B}}}{\mu_0} = \frac{\bar{\mathbf{E}}\times\overline{\Delta\mathbf{B}}}{\mu_0} + \frac{\overline{(\mathbf{E}-\bar{\mathbf{E}})\times(\Delta\mathbf{B}-\overline{\Delta\mathbf{B}})}}{\mu_0}$$

Poynting flux from the empirical model is consist of two parts: (1) Poynting flux associated with the mean electric field ($\bar{\mathbf{E}}$) and magnetic field disturbance ($\overline{\Delta\mathbf{B}}$), which are provided by the model (2) Poynting flux associated with the variabilities of the electric field and the magnetic field disturbance.

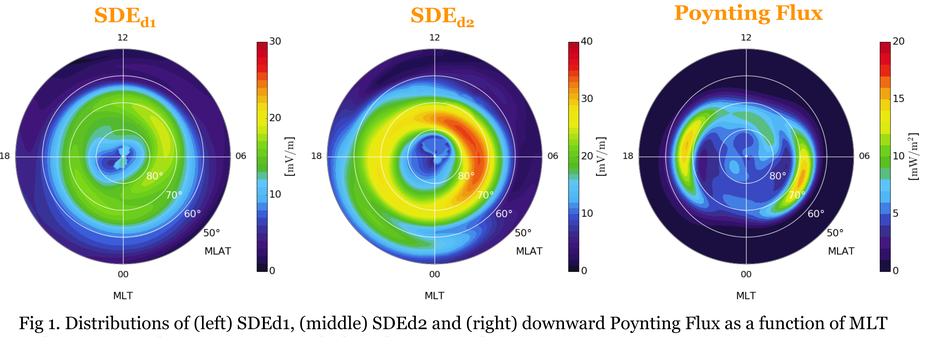

Fig 1. Distributions of (left) SDEd1, (middle) SDEd2 and (right) downward Poynting Flux as a function of MLT and MLAT at 110 km. (Bt=5 nT, IMF clock angle=180°, and sinT=0)

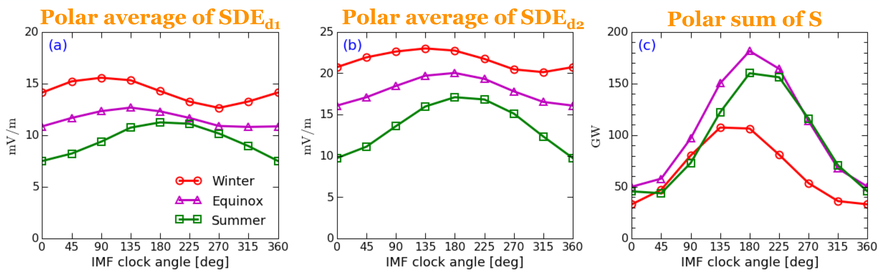

Fig 2. Polar average [above 60° MLAT] of (a) SDEd1, (b) SDEd2 and (c) polar sum [above 60° MLAT] of Poynting flux in different seasons and over a range of IMF clock angles. (Bt=5 nT, 110 km)

- SDEd1 is smaller than SDEd2 in general;
- SDEd1, SDEd2 and Poynting flux (S) exhibit seasonal variations: SDEd1 and SDEd2 maximize at winter, followed by equinox and summer, while Poynting flux tends to maximize at equinox and minimize at winter;
- SDEd1 and SDEd2 reach maximum when By is positive and has a minimum when By is negative at winter. SDEd1 at equinox also follows the same trend. SDEd2 at equinox and SDEs at summer tend to maximize when Bz is negative and dominant, which is similar as Poynting flux.

2. GITM and empirical model coupling

Deng et al. [2009] coupled the E variability from the empirical model into Thermosphere Ionosphere Electrodynamics General Circulation Model (TIEGCM) to study the impact of the E variability on thermosphere. Following Deng et al. [2009], we included the E variability from the empirical model into Global Ionosphere and Thermosphere Model (GITM) to examine the contribution of the electric variability to Joule heating. In addition, Poynting flux from the empirical model has also been compared with the Joule heating from GITM.

For GITM simulation: UT =0; Bz=-5 nT; By=0; HP =30 GW; Convection model: Weimer 2005 model; Aurora model: Fuller-Rowell and Evans model; Grid: 5° lon x 2.5° lat x 1/3 scale height in height; time step: 2s; Variability: Flip the sign of σ_E every 1 min.

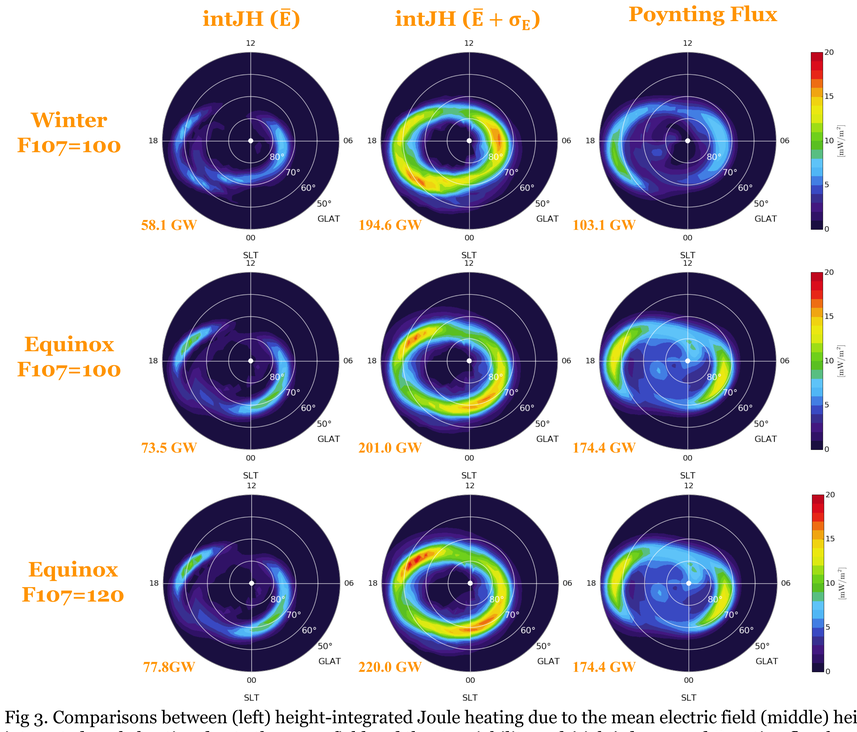

Fig 3. Comparisons between (left) height-integrated Joule heating due to the mean electric field (middle) height-integrated Joule heating due to the mean field and the E variability and (right) downward Poynting flux from the empirical model in geographic coordinate at 110 km under different conditions. The hemispheric total heating is shown at the bottom left of each plot.

- The height-integrated Joule heating exhibits a significant enhancement after including E variability, especially during the winter (enhanced by >200%).
- The intJH ($\bar{E}+\sigma_E$) at dawn-, dusk-side and cusp regions become comparable with Poynting flux, however, the Poynting flux does not exhibit large values at midnight as the intJH ($\bar{E}+\sigma_E$). In addition, Poynting flux is larger in the polar cap than the intJH ($\bar{E}+\sigma_E$).
- The hemispheric intJH ($\bar{E}+\sigma_E$) is generally larger than hemispheric Poynting flux, especially in the winter (almost twice as Poynting flux).

3. Statistical results from DMSP F15 satellite

In order to examine which one of the intJH ($\bar{E}+\sigma_E$) from GITM or Poynting flux from the empirical model can capture the characteristics of the realistic Poynting flux input, statistical results from 5-year DMSP F15 data (2000-2004) are presented here. The data presented here are from >2000 Bz negative and dominant North Pole passes at equinox and under moderate storm condition (3<Kp<6, Bz median ~-5nT, By median ~0 nT).

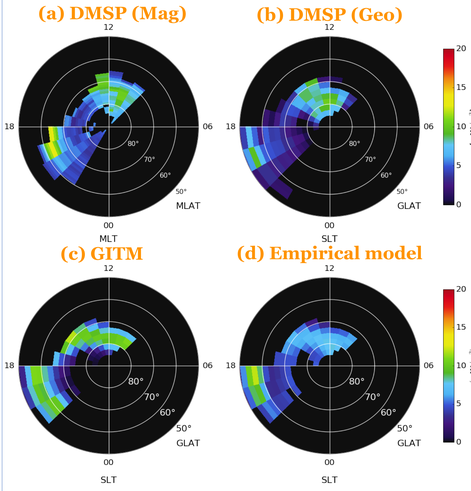

Fig 4. (a) DMSP downward Poynting flux data is binned in 1h MLT x 1° MLAT bin (b) The distribution of the downward Poynting flux in Fig 4a is converted to 1h SLT x 2.5° GLAT bin, UT = 0 (c) GITM intJH ($\bar{E}+\sigma_E$) and (d) Poynting flux shown in the bottom panel of Fig 3 are displayed in 1h SLT x 2.5° GLAT bin, only the regions where DMSP climatological values in Fig 4b are considerable are shown in Figs 4c and 4d for better comparisons. All results are mapped to 110 km.

- Climatological DMSP F15 Poynting flux shows peaks at nightside and cusp regions.
- GITM intJH ($\bar{E}+\sigma_E$) overestimates Poynting flux at nightside and cusp regions.
- The Poynting flux from the empirical model slightly overestimates the nightside Poynting flux and underestimates Poynting flux at cusp region.

4. Summary

- The empirical model shows the electric variability maximizes at winter while Poynting flux peaks at equinox.
- After adding E variability, the integrated Joule heating from GITM shows a significant enhancement as compared with that only due to the mean electric field. Although the distribution of the GITM intJH ($\bar{E}+\sigma_E$) becomes more consistent with that of Poynting flux, it is larger than Poynting flux from the empirical model, especially in winter.
- DMSP F15 observations show that large downward Poynting flux can be found at cusp and nightside regions at equinox during moderate storm and when Bz is negative and dominant. In comparison with GITM intJH ($\bar{E}+\sigma_E$) and Poynting flux from the empirical model, GITM intJH ($\bar{E}+\sigma_E$) generally overestimates the energy input at nightside and cusp regions, while empirical model slightly overestimates the Poynting flux at nightside and underestimates it at cusp.